

## Direct observation of irradiation-induced nanocavity shrinkage in Si

X. F. Zhu, J. S. Williams, M. J. Conway, M. C. Ridgway, F. Fortuna, M.-O. Ruault, and H. Bernas

Citation: *Applied Physics Letters* **79**, 3416 (2001); doi: 10.1063/1.1413497

View online: <http://dx.doi.org/10.1063/1.1413497>

View Table of Contents: <http://scitation.aip.org/content/aip/journal/apl/79/21?ver=pdfcov>

Published by the [AIP Publishing](#)

---

### Articles you may be interested in

[Temperature-dependent growth and transient state of hydrogen-induced nanocavities in silicon](#)

*J. Appl. Phys.* **104**, 034301 (2008); 10.1063/1.2960347

[On the role of nanocavities in suppressing boron transient enhanced diffusion and deactivation in F + coimplanted silicon](#)

*J. Appl. Phys.* **103**, 103525 (2008); 10.1063/1.2927391

[Cu gettering in ion implanted and annealed silicon in regions before and beyond the mean projected ion range](#)

*J. Appl. Phys.* **94**, 3834 (2003); 10.1063/1.1602951

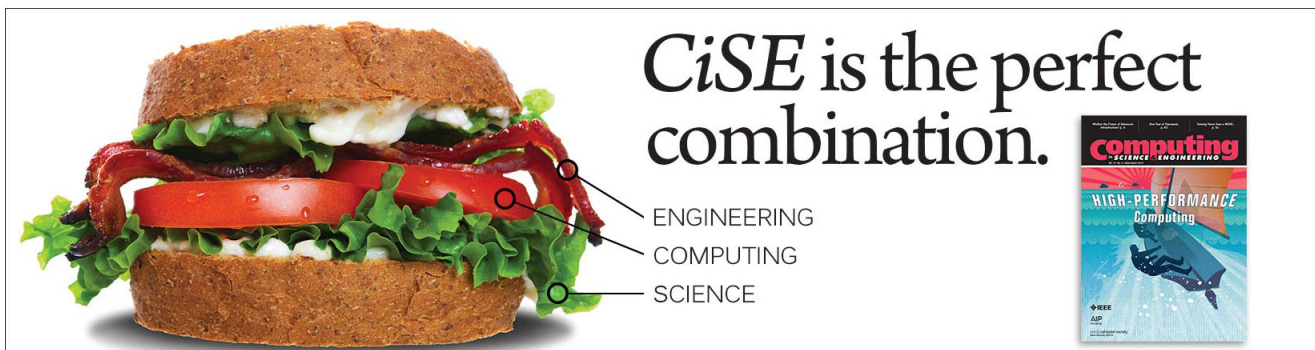
[Reply to "Comment on 'Interstitial-type defects away of the projected ion range in high energy ion implanted and annealed silicon'" \[Appl. Phys. Lett. 77, 151 \(2000\)\]](#)

*Appl. Phys. Lett.* **77**, 153 (2000); 10.1063/1.126907

[Comment on "Interstitial-type defects away from the projected ion range in high energy ion implanted and annealed silicon" \[Appl. Phys. Lett. 75, 1279 \(1999\)\]](#)

*Appl. Phys. Lett.* **77**, 151 (2000); 10.1063/1.126906

---

An advertisement for CiSE (Computing, Interdisciplinary Science, and Engineering). On the left is a large sandwich with lettuce, tomato, and meat. On the right, the text reads "CiSE is the perfect combination." Below this text are three lines: "ENGINEERING", "COMPUTING", and "SCIENCE", each with a line pointing to a part of the sandwich. To the right of the text is a small image of a journal cover titled "computing SCIENCE ENGINEERING" with the subtitle "HIGH-PERFORMANCE Computing".

## Direct observation of irradiation-induced nanocavity shrinkage in Si

X. F. Zhu,<sup>a)</sup> J. S. Williams, and M. J. Conway

*Department of Electronic Materials Engineering, Research School of Physical Sciences and Engineering, Australian National University, Canberra, Australia*

M. C. Ridgway,<sup>b)</sup> F. Fortuna, M.-O. Ruault, and H. Bernas

*Centre de Spectrometrie Nucleaire et de Spectrometrie de Masse, UMR CNRS-Universite Paris XI, Orsay, France*

(Received 11 June 2001; accepted for publication 27 August 2001)

Nanocavities in Si substrates, formed by conventional H implantation and thermal annealing, are shown to evolve in size during subsequent Si irradiation. Both *ex situ* and *in situ* analytical techniques were used to demonstrate that the mean nanocavity diameter decreases as a function of Si irradiation dose in both the crystalline and amorphous phases. Potential mechanisms for this irradiation-induced nanocavity evolution are discussed. In the crystalline phase, the observed decrease in diameter is attributed to the gettering of interstitials. When the matrix surrounding the cavities is amorphized, cavity shrinkage may be mediated by one of two processes: nanocavities can supply vacancies into the amorphous phase and/or the amorphous phase may flow plastically into the nanocavities. Both processes yield the necessary decrease in density of the amorphous phase relative to crystalline material. © 2001 American Institute of Physics.

[DOI: 10.1063/1.1413497]

Nanocavities can be readily produced in Si substrates by H or He implantation followed by thermal annealing at elevated temperatures.<sup>1</sup> The latter process induces the gaseous atoms to cluster and form bubbles then subsequently diffuse from the substrate. Dangling bonds on the internal surface of the resulting voids represent an effective trapping site for metallic impurities that degrade microelectronic device performance.<sup>2</sup> As a consequence, the formation and stability of nanocavities have been studied in detail to deduce the appropriate processing conditions for optimum metallic gettering efficiency.<sup>3</sup> Recently, we also examined the influence of nanocavities on the evolution of irradiation-induced disorder<sup>4</sup> and the stability of nanocavities in amorphous Si.<sup>5</sup> In such experiments, substrates containing voids were irradiated with Si ions. We demonstrated that depending on the irradiation temperature, nanocavities in crystalline Si are either effective trapping sites for mobile Si interstitials or nucleation sites for amorphization.<sup>4</sup> Specifically, at temperatures  $> \sim 100^\circ\text{C}$ , nanocavities getter irradiation-induced interstitials and, as a result, are surrounded by a halo of crystalline material denuded of interstitial-based dislocation loops. In contrast, at temperatures  $< \sim 25^\circ\text{C}$ , nanocavities act as preferential amorphization sites and, as a result, are surrounded by a halo of amorphous material in an otherwise crystalline matrix.<sup>4</sup> In a second experiment, samples with a continuous amorphous layer surrounding the original nanocavity band were recrystallized by solid phase epitaxy. For the given implant and annealing conditions, residual open-

volume defects were *not* observed in the recrystallized layer (as deduced by transmission electron microscopy (TEM) observations and the absence of Au gettering to depths of the original nanocavity band). Nanocavities may thus have disappeared during ion irradiation and/or solid phase epitaxy. Given the diffusivity required to fill the nanocavities during recrystallization of the amorphous layer, we speculated that the former process was most probable.<sup>5</sup> Such observations suggest that the mean nanocavity diameter should exhibit irradiation dose and temperature dependencies. Accordingly, we present herein direct evidence of *irradiation*-induced nanocavity *shrinkage* in Si substrates. We demonstrate the irradiation dose dependence and show this process is operative in both crystalline and amorphous phases.

Nanocavities were formed in (100) Si substrates by H implantation and thermal annealing ( $850^\circ\text{C}/1\text{ h}$  in Ar). Irradiation-induced nanocavity evolution was studied with both *ex situ* and *in situ* characterization techniques. For *ex situ* analysis, bulk samples were first irradiated with Si ions as functions of irradiation dose and temperature. (Specific H implantation and Si irradiation conditions are listed next for each particular experiment.) To monitor potential nanocavity shrinkage resulting from the Si irradiation, samples were then annealed ( $600^\circ\text{C}/1\text{ h}$  in Ar) to recrystallize any amorphous material, subsequently implanted with Au ions ( $80\text{ keV}/4 \times 10^{14}/\text{cm}^2$  at  $\sim 21^\circ\text{C}$ ) and, finally, annealed again ( $850^\circ\text{C}/1\text{ h}$  in Ar) to diffuse Au to residual trapping sites. As previously established,<sup>6,7</sup> Au gettering is an effective and selective detector of open-volume defects in crystalline Si. Au gettering to depths of the nanocavity band was then quantified with He-ion Rutherford backscattering spectrometry (RBS) ( $2\text{ MeV}/110^\circ$  scattering) as a means of establishing the presence and extent of residual open-volume defects. Selected samples were also characterized with TEM. For *in situ* analysis, cross section TEM samples were first prepared

<sup>a)</sup>Current address: Materials Research Laboratory and Department of Electrical and Computer Engineering, University of Illinois at Urbana-Champaign, Urbana, Illinois.

<sup>b)</sup>Permanent address: Department of Electronic Materials Engineering, Research School of Physical Sciences and Engineering, Australian National University, Canberra, Australia; author to whom all correspondence should be addressed; electronic mail: mcr109@rphysse.anu.edu.au

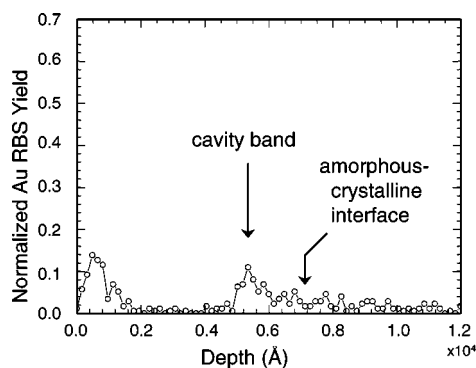


FIG. 1. Random RBS spectrum of the implanted Au depth distribution for a Si substrate containing nanocavities following Si irradiation, recrystallization, Au implantation, and annealing. Nanocavities were formed by  $50 \text{ keV}/3 \times 10^{16}/\text{cm}^2$  H implantation at  $21^\circ\text{C}$ . Substrates were irradiated with  $360 \text{ keV}/2 \times 10^{15}/\text{cm}^2$  Si ions at  $\sim -197^\circ\text{C}$ . Samples were then further annealed at  $600^\circ\text{C}$  for 1 h, implanted with  $80 \text{ keV}/4 \times 10^{14}$  Au ions at  $21^\circ\text{C}$ , then annealed again at  $850^\circ\text{C}$  for 1 h.

from bulk substrates containing nanocavities. Samples were then irradiated in the microscope (operating at 120 kV) with Si ions (100 keV at  $\sim 21^\circ\text{C}$ ) as a function of dose. Irradiation-induced nanocavity evolution was thus measurable directly without the need for Au implantation and annealing. Note that for *in situ* analyses, the Si projected range ( $\sim 150 \text{ nm}$ ) exceeded the TEM sample thickness ( $\sim 70 \text{ nm}$ ).

Figure 1 shows random RBS results for a Si substrate containing nanocavities that was first irradiated with Si ions at  $\sim -197^\circ\text{C}$ , subsequently recrystallized at  $650^\circ\text{C}$ , then implanted with Au ions and thermally annealed. Note that the depth of the original nanocavity band was  $\sim 500 \text{ nm}$  and that the Si irradiation produced a continuous amorphous layer from the surface to a depth of  $\sim 700 \text{ nm}$ . Figure 1 shows that Au is gettered to depths of  $< 100 \text{ nm}$  (the surface and Au implant disorder),  $\sim 500 \text{ nm}$  (residual open-volume defects), and  $600\text{--}800 \text{ nm}$  (end-of-range disorder). TEM indicated that the gettering sites below the surface were most likely nanocavities (filled with Au) and dislocations, the latter in close proximity to the original amorphous/crystalline interface produced by the Si irradiation. (Indeed, previous studies<sup>6,7</sup> have shown that when the available Au concentration is high and the residual open volume is small, Au will completely fill voids upon annealing.) These results demonstrate that nanocavities can be partially retained in amorphous Si under the given irradiation conditions and are not eliminated during solid phase epitaxy. In control samples which were not irradiated with Si ions, all the implanted Au was gettered to the nanocavity band. The results of Fig. 1 are thus indicative of a reduction in nanocavity volume and/or competition from the alternative Au trapping sites at the surface and end of range. The reduction in nanocavity volume most likely occurs during Si irradiation but shrinkage during thermal annealing cannot be completely discounted though our previous diffusivity arguments<sup>5</sup> suggest it is highly improbable.

For a second experiment, Si substrate containing nanocavities was irradiated with Si ions  $\sim 21^\circ\text{C}$ . As anticipated, irradiation-induced disorder in the substrate (in the form of displaced lattice atoms) increased as a function of Si dose. The formation of a buried amorphous layer, centered at the

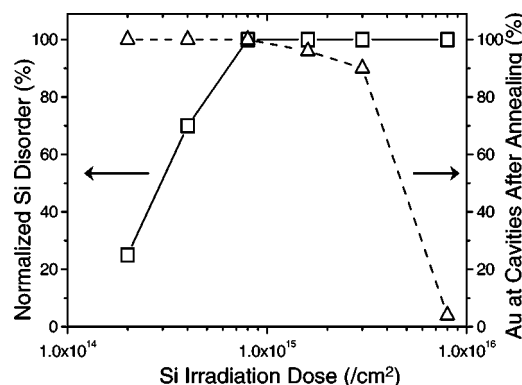


FIG. 2. Si disorder before recrystallization and Au getter efficiency after thermal annealing, all as a function of Si ion dose. Nanocavities were formed by  $20 \text{ keV}/2 \times 10^{16}/\text{cm}^2$  H implantation at  $21^\circ\text{C}$ . Substrates were irradiated with  $245 \text{ keV}$  Si ions at  $\sim 21^\circ\text{C}$ . Samples were then further annealed at  $600^\circ\text{C}$  for 1 h, implanted with  $80 \text{ keV}/4 \times 10^{14}$  Au ions at  $21^\circ\text{C}$ , then annealed again at  $850^\circ\text{C}$  for 1 h.

nanocavity band, was evident for an irradiation dose of  $8 \times 10^{14}/\text{cm}^2$ . RBS measurements were also performed on the same samples after recrystallization, subsequent Au implantation and thermal annealing, to detect residual open-volume defects as monitored by Au gettering. Figure 2 compares Si irradiation-induced disorder (before recrystallization) and Au gettering (after annealing), both at the depth of the original nanocavity band. For Si irradiation doses below the amorphization threshold ( $< 8 \times 10^{14}/\text{cm}^2$ ), no change in Au gettering efficiency is apparent. However, such results do *not* preclude irradiation-induced nanocavity shrinkage—should the areal concentration of nanocavity gettering sites still exceed the Au ion dose, a change in Au gettering efficiency may not be measurable. For Si irradiation doses of  $8\text{--}30 \times 10^{14}/\text{cm}^2$ , Fig. 2 again demonstrates that open-volume defects remain following amorphization by Si irradiation and subsequent solid phase epitaxy (as indicated by  $> 90\%$  of Au gettered to depths of the original nanocavity band). In contrast, for the highest Si irradiation dose ( $8 \times 10^{15}/\text{cm}^2$ ), no Au gettering to depths of the original nanocavity band was measurable, indicative of the absence of residual open-volume defects. We suggest the results of Fig. 2 are consistent with an irradiation dose dependent reduction in Au gettering sites or, specifically, a reduction in nanocavity diameter and/or nanocavity concentration. Furthermore, the rate of nanocavity shrinkage is apparently much enhanced in the amorphous phase. Comparing results for irradiation temperatures of  $\sim -197$  and  $\sim 21^\circ\text{C}$  (not shown), a significant temperature dependence was not measurable.

Figure 3 shows *in situ* TEM micrographs of a single nanocavity during Si irradiation at  $\sim 21^\circ\text{C}$ . As is readily apparent, the mean nanocavity diameter decreases as a function of Si irradiation dose. Preferential amorphization of the Si substrate in close proximity to the nanocavity is evident for a Si ion dose of  $2 \times 10^{15}/\text{cm}^2$  (as is consistent with our previous report).<sup>4</sup> At greater ion doses, the Si surrounding the nanocavity is completely amorphized. The crystalline-to-amorphous transformation of the Si substrate is thus concomitant with the irradiation-induced nanocavity evolution. The greatest change in nanocavity diameter occurs following amorphization. We also note that the change in nanocavity volume following amorphization is not proportional to irra-



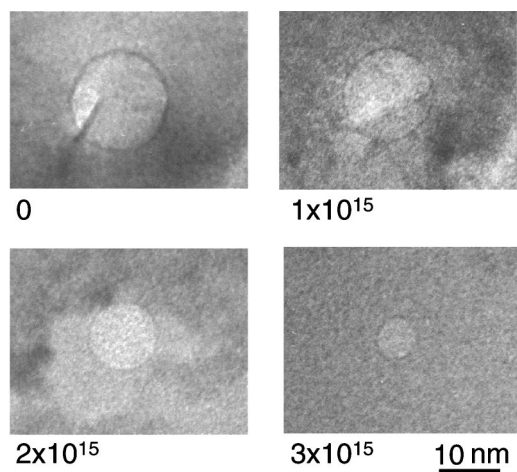


FIG. 3. *in situ* TEM micrographs of a single nanocavity for an irradiation temperature of  $\sim 21$  °C as a function of Si ion dose ( $\text{cm}^2$ ).

diation dose, since a much greater rate of change in mean nanocavity diameter is anticipated as the nanocavity dimensions decrease. Though detailed measurements with a statistically meaningful number of nanocavities<sup>8</sup> are necessary to accurately determine the irradiation-parameter dependencies, the *in situ* results readily demonstrate that irradiation-induced nanocavity shrinkage is operative in both crystalline and amorphous Si, but is considerably more pronounced in the latter phase.

Mechanisms for the irradiation-induced decrease in the mean nanocavity diameter may now be considered. In the crystalline phase, the diffusivity of a self-interstitial significantly exceeds that of a vacancy<sup>9</sup> and the former is further enhanced under ion irradiation.<sup>10</sup> Nanocavities effectively getter irradiation-induced interstitials<sup>4,11</sup> as is consistent with the nongas-filled, vacuum environment of such voids. The result of interstitial gettering is a reduction in nanocavity diameter. In the amorphous phase, binding energies to nanocavity internal surfaces and point-defect-like diffusivities and concentrations are modified. For example, an enhanced equilibrium vacancy concentration in the amorphous phase is evidenced by an increased metal and H solubility.<sup>12</sup> In contrast, self-interstitial mobility is potentially retarded relative to the crystalline phase as such defects are readily annihilated by small adjustments with neighboring atoms.<sup>13</sup> Specifically, computer simulations of irradiation-induced vacancies and interstitials in an amorphous solid demonstrated that vacancies were more readily accommodated (or equivalently, less readily annihilated) in the amorphous matrix.<sup>14</sup> During ion irradiation, nanocavities in the amorphous phase may thus act as a vacancy source, not as an interstitial sink. (This presupposes that such vacancies are mobile in amorphous Si under ion irradiation.) There is clear evidence that amor-

phous Si flows during ion irradiation at room temperature.<sup>15</sup> This may provide the mechanism for redistributing the nanocavity open volume throughout the surrounding amorphous matrix during ion irradiation. Given amorphous Si is  $\sim 2\%$  less dense than crystalline Si,<sup>16</sup> plastic flow or vacancy accommodation in the amorphous phase may enable amorphous Si to achieve such a density and, at the same time, yield nanocavity shrinkage. In light of this proposal, it is interesting to contemplate the precise mechanism for irradiation-induced plastic flow and how the amorphous material responds around individual ion tracks. Detailed *in situ* measurements of nanocavity diameter as functions of irradiation dose and temperature are required to deduce the details of such processes.

In conclusion, both *ex situ* and *in situ* analytical techniques have been utilized to demonstrate irradiation-induced nanocavity shrinkage in Si substrates. The mean nanocavity diameter decreases as a function of irradiation dose in both crystalline and amorphous Si, but more rapidly in the latter phase. Nanocavities can be retained after solid phase epitaxy of irradiated, amorphous Si though prolonged irradiation completely removes nanocavities. Mechanisms for nanocavity evolution are suggested and the observed decrease in diameter is attributed to the gettering of self-interstitials in the crystalline phase and to vacancy release from nanocavities and/or plastic flow in the amorphous phase.

<sup>1</sup>C. C. Griffioen, J. H. Evans, P. C. de Jong, and A. van Veen, Nucl. Instrum. Methods Phys. Res. B **27**, 417 (1987).

<sup>2</sup>S. M. Myers, M. Seibt, and W. Schroter, J. Appl. Phys. **88**, 3795 (2000) and references therein.

<sup>3</sup>S. E. Donnelly, V. M. Vishnyakov, R. C. Birtcher, and G. Carter, Nucl. Instrum. Methods Phys. Res. B **132**, 175 (2001).

<sup>4</sup>J. S. Williams, X. F. Zhu, M. C. Ridgway, M. J. Conway, B. C. Williams, F. Fortuna, M.-O. Ruault, and H. Bernas, Appl. Phys. Lett. **77**, 4280 (2000).

<sup>5</sup>X. F. Zhu, J. S. Williams, D. J. Llewellyn, and J. C. McCallum, Appl. Phys. Lett. **74**, 2313 (1999).

<sup>6</sup>J. S. Williams, M. J. Conway, B. C. Williams, and J. Wong-Leung, Appl. Phys. Lett. **78**, 2867 (2001).

<sup>7</sup>V. C. Venezia, D. J. Eaglesham, T. E. Haynes, A. Agarwal, D. C. Jacobson, H.-J. Gossman, and F. Baumann, Appl. Phys. Lett. **73**, 2980 (1998).

<sup>8</sup>M. C. Ridgway, M.-O. Ruault, F. Fortuna, H. Bernas, X. F. Zhu, J. S. Williams, and M. J. Conway (unpublished).

<sup>9</sup>G. S. Oehrlein, I. Krafcsik, J. L. Lindstrom, A. E. Jaworowski, and J. W. Corbett, J. Appl. Phys. **54**, 179 (1983).

<sup>10</sup>A. Hallen, N. Keskitalo, L. Josyula, and B. G. Svensson, J. Appl. Phys. **86**, 214 (1999).

<sup>11</sup>V. Raineri and U. Campisano, Nucl. Instrum. Methods Phys. Res. B **120**, 56 (1996).

<sup>12</sup>D. C. Jacobson, R. G. Elliman, J. M. Gibson, G. L. Olson, J. M. Poate, and J. S. Williams, Mater. Res. Soc. Symp. Proc. **74**, 327 (1987).

<sup>13</sup>B. T. A. Chang and J. C. M. Li, Scr. Metall. **11**, 933 (1991).

<sup>14</sup>T. K. Chaki and J. C. M. Li, Philos. Mag. B **51**, 557 (1985).

<sup>15</sup>C. A. Volkert, J. Appl. Phys. **70**, 3521 (1991).

<sup>16</sup>S. Roorda, L. Cliché, M. Chicoine, and R. A. Massut, Nucl. Instrum. Methods Phys. Res. B **106**, 80 (1995).